

Retinal Gene Expression and Müller Cell Responses after Branch Retinal Vein Occlusion in the Rat

Matus Rehak,¹ Margrit Hollborn,^{1,2} Ianors Iandiev,^{1,3} Thomas Pannicke,⁴ Anett Karl,⁴ Antje Wurm,⁴ Leon Kohen,^{1,5} Andreas Reichenbach,⁴ Peter Wiedemann,¹ and Andreas Bringmann¹

PURPOSE. In a rat model of branch retinal vein occlusion (BRVO), changes in gene expression of factors implicated in the development of retinal edema and alterations in the properties of Müller cells were determined.

METHODS. In adult Long-Evans rats, BRVO was induced by laser photocoagulation of retinal veins; untreated eyes served as controls. The mRNA levels of after factors were determined with real-time RT-PCR in the neural retina and retinal pigment epithelium after 1 and 3 days of BRVO: VEGF-A, pigment epithelium-derived factor (PEDF), tissue factor, prothrombin, the potassium channel Kir4.1, and aquaporins 1 and 4. Potassium currents were recorded in isolated Müller cells, and cellular swelling was assessed in retinal slices.

RESULTS. In the neural retina, the expression of VEGF was upregulated within 1 day of BRVO and returned to the control level after 3 days. PEDF was upregulated in the neuroretina and retinal pigment epithelium after 3 days of BRVO. Prothrombin, Kir4.1, and both aquaporins were downregulated in the neuroretina. After BRVO, Müller cells displayed a decrease in their potassium currents and an altered distribution of Kir4.1 protein, an increase in the size of their somata, and cellular swelling under hyposmotic stress that was not observed in control tissues.

CONCLUSIONS. BRVO results in a rapid transient increase in the expression of VEGF and a delayed increase in the expression of PEDF. The downregulation of Kir4.1 and aquaporins, the mislocation of Kir4.1 protein, and the osmotic swelling of Müller cells may contribute to the development of edema and neuronal degeneration. (*Invest Ophthalmol Vis Sci.* 2009;50:2359–2367) DOI:10.1167/iovs.08-2332

In addition to retinal capillary nonperfusion and hemorrhage, macular edema is a major cause of vision loss in patients with central retinal vein occlusion (CRVO) and branch retinal vein occlusion (BRVO).^{1–3} A primary mechanism of edema formation is the breakdown of the blood-retinal barrier formed by vascular endothelial and retinal pigment epithelial (RPE) cells. Vascular endothelial growth factor (VEGF), which is upregulated during retinal ischemia,⁴ is a key player in increasing the permeability of the blood-retinal barrier.^{5,6} The intraocular level of VEGF is increased in patients with macular edema with BRVO and is correlated with the size of the nonperfusion area and the severity of edema.⁷ Intravitreal administration of VEGF inhibitors have been shown in some studies to be effective in improving visual acuity and reducing macular thickness in CRVO and BRVO,² suggesting that excess production of VEGF contributes to the development of macular edema.^{8,9} It has been shown that the expression of VEGF is negatively regulated by antiangiogenic factors such as the pigment epithelium-derived factor (PEDF).^{10,11} In addition to other inflammatory factors,¹² the proinflammatory protease thrombin may be involved in the development of tissue edema. Thrombin is generated from extravasated prothrombin in areas of hemorrhage. Whether prothrombin is also produced in the retina remains to be determined. It is known that thrombin exerts multiple effects on RPE cells, including formation of intercellular gaps and expression of VEGF.^{13,14} Blood coagulation in areas of tissue damage and hemorrhage is initiated by the exposure of tissue factor.¹⁵ However, it is not known whether various factors that modulate blood-retinal barrier permeability, such as VEGF, PEDF, prothrombin, and tissue factor, are altered in their expression after BRVO and whether the alterations are time dependent. Therefore, we investigated the retinal gene expression of these factors in a rat model of BRVO.

In addition to the increase in blood-retinal barrier permeability, impairment in fluid clearance from the retinal tissue may contribute to the development of retinal edema.^{16,17} The absorption of excess water from the retinal tissue is carried out by RPE and Müller glial cells. RPE cells dehydrate the subretinal space, whereas Müller cells dehydrate the inner retinal tissue.^{17,18} Water clearance from the retinal tissue is mediated by an osmotically driven transcellular water transport that is coupled to a transport of potassium and chloride ions.^{18,19} Water flow through the membranes of Müller and RPE cells is facilitated by water-selective channels, the aquaporins. Photoreceptors and RPE cells express aquaporin-1, whereas the major water channel of Müller cells is aquaporin-4.^{20–22} Colocalization of aquaporin-4 with the inwardly rectifying potassium (Kir) channel Kir4.1 in distinct membrane domains of Müller cells has led to the suggestion that water transport is coupled to the spatial-buffering potassium currents flowing through Müller cells.²² Dysregulation of the transglial water transport after downregulation of Kir4.1 channels and osmotic swelling of Müller cells (cytotoxic edema) under pathologic conditions such as transient retinal ischemia-reperfusion and diabetes have been implicated in the development of retinal edema.^{17,23,24} Therefore, we also investigated whether the

From the ¹Department of Ophthalmology and Eye Hospital, the ²Interdisciplinary Center of Clinical Research, the ³Translational Center for Regenerative Medicine, and the ⁴Paul Flechsig Institute of Brain Research, University of Leipzig, Leipzig, Germany; and the ⁵Helios Klinikum Aue, Aue, Germany.

Supported by grants from the Bundesministerium für Bildung und Forschung (1113MB, DLR/OIGZ0703), the Interdisciplinary Center of Clinical Research at the University of Leipzig Faculty of Medicine (C35, Z10), and the Deutsche Forschungsgemeinschaft (KO 1547/6–1, GRK 1097/1).

Submitted for publication May 25, 2008; revised September 2, 2008; accepted March 11, 2009.

Disclosure: **M. Rehak**, None; **M. Hollborn**, None; **I. Iandiev**, None; **T. Pannicke**, None; **A. Karl**, None; **A. Wurm**, None; **L. Kohen**, None; **A. Reichenbach**, None; **P. Wiedemann**, None; **A. Bringmann**, None

The publication costs of this article were defrayed in part by page charge payment. This article must therefore be marked “advertisement” in accordance with 18 U.S.C. §1734 solely to indicate this fact.

Corresponding author: Matus Rehak, Department of Ophthalmology and Eye Hospital, University of Leipzig Faculty of Medicine, Liebigstrasse 10–14, 04103 Leipzig, Germany; matus.rehak@medizin.uni-leipzig.de.

expression and localization of Kir4.1 and aquaporin-4 are altered after BRVO.

MATERIALS AND METHODS

Materials

Chloromethyltetramethylrosamine (Mitotracker Orange) was purchased from Molecular Probes (Eugene, OR). Papain was from Roche (Mannheim, Germany). DNase I, prostaglandin E₂, 4-bromophenacyl bromide, indomethacin, dithiothreitol, and all other substances used were obtained from Sigma-Aldrich (Taufkirchen, Germany).

Experimental BRVO

All procedures concerning animals were performed in accordance with applicable German laws and the ARVO Statement for the Use of Animals in Ophthalmic and Vision Research. Adult pigmented Long-Evans rats (250–350 g) were used. The animals were reared in 12-hour (6:00 am–6:00 pm) light/dark cycles. Animals were anesthetized by intramuscular ketamine (100 mg/kg; Ketamin; Inresa, Freiburg, Germany) and xylazine (5 mg/kg; Rompur; Bayer, Leverkusen, Germany). In one eye of each animal, branch retinal veins near the optic nerve head were photocoagulated 15 minutes after intraperitoneal injection of 0.2 mL of 10% sodium fluorescein with a blue-green argon laser and the aid of a 78-diopter lens (1 second, 50 μ m, 50–100 mW, 5–12 spots per vein). Contralateral eyes remained untreated and served as controls. In 24 animals, all retinal veins of one eye were occluded. In another five animals, half the retinal branch veins were occluded while the other veins remained perfused. One day after laser photocoagulation, the success of vein occlusion was proved by indirect stereoscopic ophthalmoscopy and fluorescein angiography with intravenous injection of 0.1 mL of 10% sodium fluorescein. The animals were killed with carbon dioxide at different time periods after BRVO, and the eyes were removed.

Real-Time PCR

Preparation of total RNA from the neuroretina and retinal pigment epithelium and real-time PCR were conducted using standard methods described in the Supplement, online at <http://www.iovs.org/cgi/content/full/50/5/2359/DC1>. PCR was carried out using primer pairs described in the Supplement. mRNA expression was normalized to the levels of β -actin mRNA.

Electrophysiological Recordings

Müller cells were acutely isolated from pieces of retinal tissue according to a method described in the Supplement. Whole-cell membrane currents were recorded in Müller cells isolated from tissues in which all veins were occluded and from retinas of untreated control eyes. The experiments were performed at room temperature (22°C–25°C). Currents were recorded using an amplifier (Axopatch 200A; Axon Instruments, Foster City, CA) and a computer program (ISO-2; MFK, Niedernhausen, Germany). Patch pipettes were pulled from borosilicate glass (Science Products, Hofheim, Germany) and had resistances between 4 and 6 M Ω when filled with the intracellular solution that contained 10 mM NaCl, 130 mM KCl, 1 mM CaCl₂, 2 mM MgCl₂, 10 mM EGTA, and 10 mM HEPES-Tris (pH 7.1). Signals were low-pass filtered at 1, 2, or 6 kHz (eight-pole Bessel filter) and digitized at 5, 10, or 30 kHz, respectively, using a 12-bit A/D converter. The recording chamber was continuously perfused with extracellular solution that contained 135 mM NaCl, 3 mM KCl, 2 mM CaCl₂, 1 mM MgCl₂, 1 mM Na₂HPO₄, 10 mM HEPES, and 11 mM glucose equilibrated to pH 7.4 with Tris.

To evoke membrane currents, depolarizing and hyperpolarizing voltage steps of 250-ms duration, with increments of 10 mV, were applied from a holding potential of –80 mV (which is near the resting membrane potential of the cells; see Fig. 3C). To isolate fast transient A-type potassium currents, two voltage step protocols were used in the

presence of the Kir channel blocker barium chloride (100 μ M): depolarizing steps (i) after maximal activation of these currents by a 500-ms prepulse to –120 mV and (ii) after steady state inactivation of the currents by a 500-ms prepulse to –40 mV. The currents obtained with both protocols were subtracted (i – ii), and, if present, fast transient A-type currents became visible whereas delayed rectifier potassium currents were eliminated. Membrane capacitance of the cells was measured by the integral of the uncompensated capacitive artifact (filtered at 6 kHz) evoked by a hyperpolarizing voltage step from –80 to –90 mV in the presence of extracellular barium chloride (1 mM). Resting membrane potential was measured in the current-clamp mode.

Müller Cell Swelling

To determine the volume changes of Müller glial cells evoked by hypoosmotic stress, the cross-sectional area of Müller cell somata in the inner nuclear layer of retinal slices was measured.²³ Acutely isolated retinal slices (thickness, 1 mm) were made from the freshly prepared retinal tissue, placed in a perfusion chamber, and loaded with the vital dye (10 μ M; Mitotracker Orange; Molecular Probes). It has been shown that this dye is taken up (in addition to photoreceptor segments) selectively by Müller cells in the retina, whereas neurons, photoreceptor cell bodies, astrocytes, and microglial cells remain unstained.²⁵ The stock solution of the dye was prepared in dimethyl sulfoxide and resolved in extracellular solution that contained 136 mM NaCl, 3 mM KCl, 2 mM CaCl₂, 1 mM MgCl₂, 10 mM HEPES-Tris, and 11 mM glucose, adjusted to pH 7.4 with Tris. A gravity-fed system with multiple reservoirs was used to perfuse the recording chamber continuously with extracellular solutions; the hypoosmolar solution and test substances were added by rapid changing of the perfusate. The hypoosmolar solution contained 60% of control osmolarity and was made by adding distilled water to the extracellular solution. Barium chloride (1 mM) was preincubated for 10 minutes in extracellular solution before it was applied within the hypoosmolar solution. Blocking substances were preincubated for 15 minutes before hypoosmotic challenge. Slices were examined using an upright confocal laser scanning microscope (LSM 510 Meta; Zeiss, Oberkochen, Germany) and a water immersion objective (Achromplan 63x/0.9; Zeiss). The pinhole was set at 172 μ m, and the thickness of the optical section was adjusted to 1 μ m. Vital dye (Mitotracker Orange; Molecular Probes) was excited at 543 nm, and emission was recorded with a 560-nm long-pass filter. In the course of the experiments, the vital dye-stained somata of Müller cells were recorded at the plane of their maximal extension. To ensure that the maximum soma areas were precisely recorded, the focal plane was continuously adjusted in the course of the experiments. Stained cell bodies from the surfaces of the slices up to a depth of approximately 20 μ m were recorded.

Immunostaining

Slices of isolated retinas were immunostained using a standard method described in the Supplement. The following antibodies were used: mouse anti-vimentin (1:200; V9 clone, Santa Cruz), rabbit anti-glial fibrillary acidic protein (GFAP; 1:200; Dako), rabbit anti-Kir4.1 (1:200; Alomone Laboratories), rabbit anti-rat aquaporin-4 (1:200; Sigma), Cy3-conjugated goat anti-rabbit IgG (1:400; Dianova), and Cy2-coupled goat anti-mouse IgG (1:200; Dianova).

Statistical Analysis

To determine the extent of swelling of Müller cell somata, the cross-sectional area of vital dye (Mitotracker Orange; Molecular Probes)-stained cell bodies in the inner nuclear layer of retinal slices was measured offline using the image analysis software of the laser scanning microscope. Bar diagrams (see Fig. 6) display the mean cross-sectional areas of Müller cell somata measured after 4-minute perfusion of the hypoosmolar solution, in percentage of the soma area measured before osmotic challenge (100%). The amplitude of the inward potassium (Kir) currents was measured at the end of the 250-ms voltage step from –80 to –140 mV. Statistical analysis was made using commercial

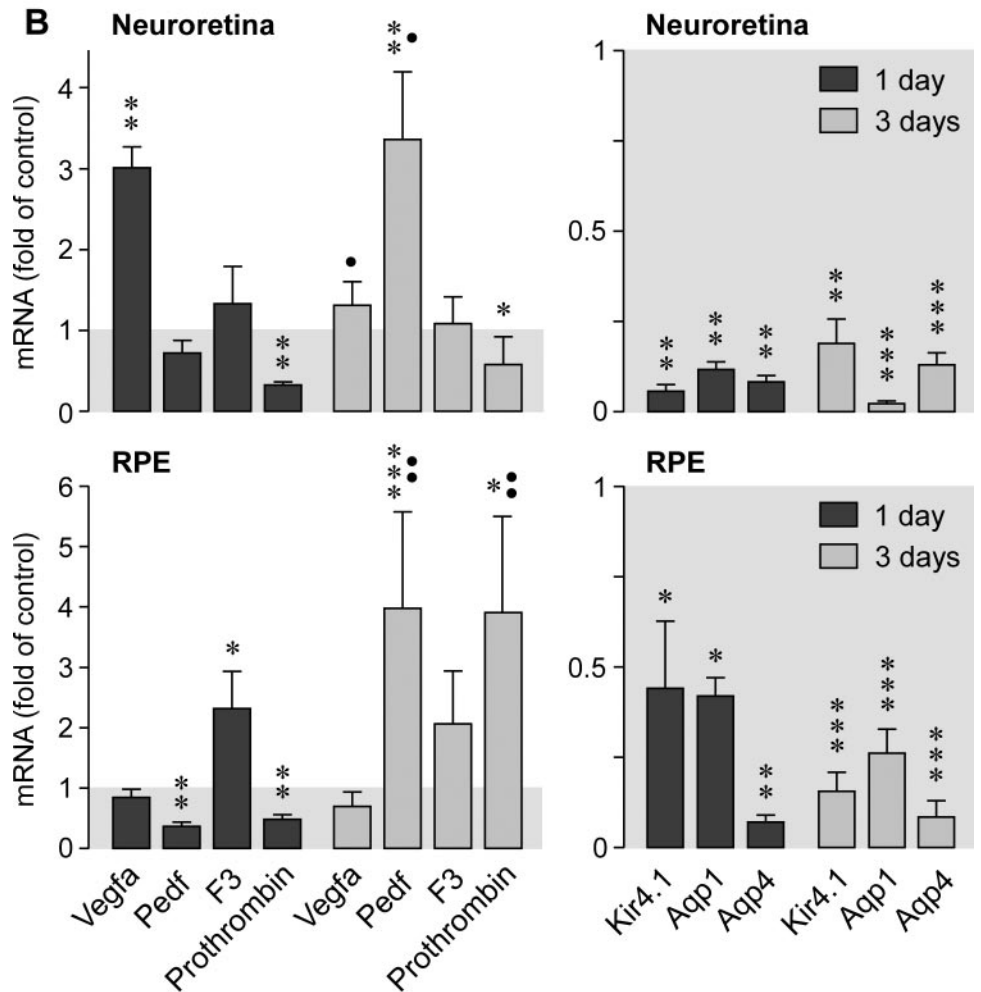
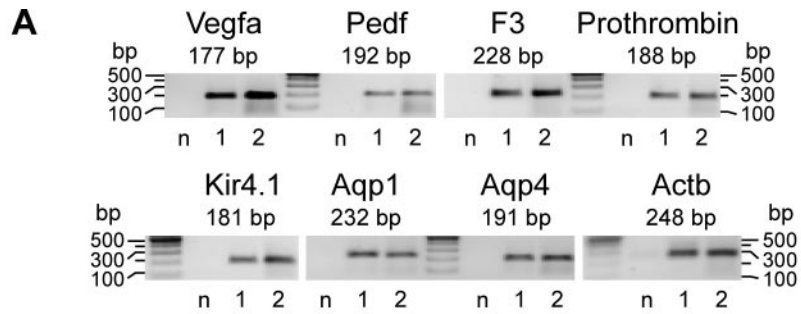


FIGURE 1. Alterations in retinal gene expression after BRVO of factors and channels implicated in the development/resolution of edema and in retinal osmoregulation. (A) mRNA expression in the neuroretina and RPE from a control eye for the following proteins: VEGF-A (Vegfa), PEDF (Pedf), tissue factor (F3), prothrombin, Kir4.1, aquaporin-1 (Aqp1), aquaporin-4 (Aqp4), and β -actin (Actb). Ethidium bromide-stained agarose gels of the PCR amplicons are shown. Each reaction product yielded a single band that was confirmed by melting curve analysis (not shown). n, negative control; 1, RPE; 2, neuroretina. Negative controls were made by adding double-distilled water instead of cDNA as template. (B) Time-dependent alterations in the gene expression as revealed by real-time PCR analysis. Data were obtained in the neuroretina (above) and retinal pigment epithelium (below) 1 ($n = 5$) and 3 days ($n = 6$) after BRVO and are expressed in relation to the values obtained in tissues from contralateral untreated control eyes. Significant differences compared with control: * $P < 0.05$; ** $P < 0.01$; *** $P < 0.001$. Significant differences between 1 and 3 days: • $P < 0.05$; •• $P < 0.01$.

software (SigmaPlot [SPSS Inc., Chicago, IL]; Prism program [Graphpad Software, San Diego, CA]); significance was determined by the Mann-Whitney U test for two groups, Kruskal-Wallis test followed by Dunn comparison for multiple groups, and Fisher exact test. Data are expressed as mean \pm SD (PCR, electrophysiological data) and mean \pm SEM (cell swelling data), respectively.

RESULTS

Retinal Gene Expression

We investigated the alterations in retinal gene expression of factors implicated in the development/resolution of edema. mRNA levels for the factors were determined in the neuroretina and retinal pigment epithelium after 1 and 3 days of BRVO. Neuroretinas and retinal pigment epithelium from con-

trol eyes expressed mRNA for the following factors: VEGF-A, PEDF, tissue factor, and prothrombin (Fig. 1A). Within 1 day of BRVO, VEGF was significantly ($P < 0.01$) upregulated in the neuroretina, whereas VEGF expression was not altered in the retinal pigment epithelium (Fig. 1B), suggesting selective hypoxia of the inner retina. Within 3 days of BRVO, VEGF expression in the neuroretina returned to control level. PEDF displayed a delayed upregulation in the neuroretina—that is, the expression level was unaltered after 1 day of BRVO and increased significantly ($P < 0.01$) within 3 days (Fig. 1B). In the retinal pigment epithelium, PEDF was downregulated within 1 day and upregulated after 3 days of BRVO. The expression of the tissue factor remained unaltered in the neuroretina after BRVO but was slightly increased in the retinal pigment epithelium. Prothrombin was significantly downregulated in the neuroretina after BRVO. In the retinal pigment epithelium, pro-

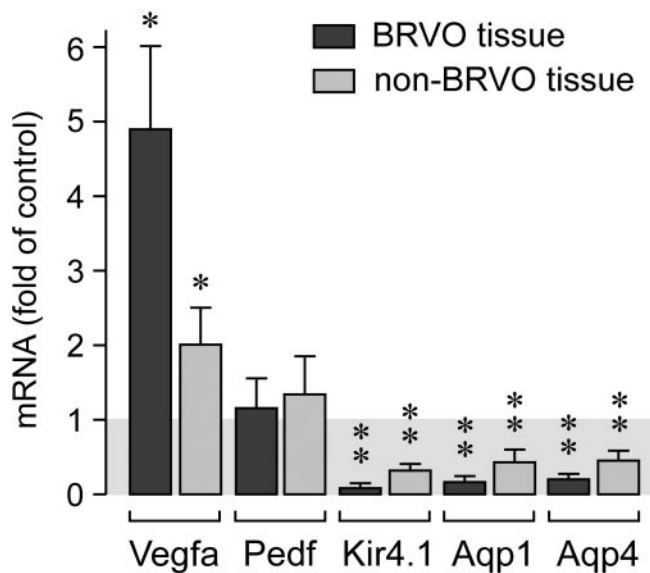


FIGURE 2. Alterations in retinal gene expression occur in vein-occluded and nonoccluded retinal areas. Data were obtained after 1 day of BRVO from neuroretinas of eyes in which half the retinal branch veins were occluded (BRVO tissue) while the other veins remained perfused (non-BRVO tissue). Data were obtained in five animals and are expressed in relation to the values obtained in tissues from contralateral untreated control eyes. Significant differences versus control: * $P < 0.05$; ** $P < 0.01$.

thrombin expression was decreased within 1 day and increased after 3 days of BRVO compared with controls (Fig. 1B). The data suggest that BRVO results in a rapid transient increase in VEGF expression and a delayed upregulation of PEDF in the neural retina.

We also investigated alterations in the retinal gene expression of potassium and water channels implicated in retinal osmoregulation. Neuroretinas and retinal pigment epithelium from control eyes expressed mRNA for the following channels: Kir4.1, aquaporin-1, and aquaporin-4 (Fig. 1A). The gene expression of these potassium and water channels decreased strongly in both tissues compared with control (Fig. 1B). This decrease was observed after 1 and 3 days of BRVO. The data suggest rapid downregulation of potassium and water channels in the retina after BRVO that might have contributed to impairment of the retinal osmoregulation.

In other animals, we investigated whether BRVO in half a retina resulted in gene expression alterations in the other half retina in which the veins remained perfused. After 1 day of BRVO, VEGF was upregulated in the vein occluded and non-occluded retinal areas, though the increase in VEGF expression was less pronounced in nonoccluded areas than in occluded areas (Fig. 2). On the other hand, the gene expression of PEDF remained unaltered in both retinal areas after 1 day of BRVO. Potassium and water channels were downregulated in occluded and nonoccluded retinal areas, with a slightly lower decrease in gene expression in the nonoccluded areas (Fig. 2). The data suggest that the gene expression alterations are not restricted to retinal areas of vein occlusion but spread into the surrounding nonoccluded tissue.

Membrane Characteristics of Müller Cells

Kir channels mediate the spatial buffering potassium currents through Müller cells necessary for the maintenance of the extracellular potassium homeostasis in the retina.²⁶ Müller cells freshly isolated from BRVO retinas displayed a severe reduction in the amplitude of the potassium currents across

their plasma membranes; especially the inward currents (which are mediated predominantly by Kir4.1)²⁶ were almost completely absent after BRVO (Fig. 3A). There was a time-dependent decrease in the Kir current amplitude of Müller cells after BRVO (Fig. 3B); the amplitude decreased to $5.2\% \pm 4.2\%$ of control within 4 days of BRVO ($P < 0.001$). It is known that the expression of Kir channels is a precondition for the negative resting membrane potential of Müller cells.²⁶ Müller cells isolated from retinas 3 and 4 days after BRVO displayed significant depolarization to approximately -50 mV compared with cells from control retinas that had a mean membrane potential of approximately -80 mV (Fig. 3C). A decrease of Kir currents in Müller cells of the rat under pathologic conditions is regularly accompanied by an increase in the incidence of cells that display transient A-type, outwardly rectifying potassium currents (Fig. 3F).^{24,27} Only a small subpopulation of Müller cells from control retinas displayed A-type currents, whereas this current type could be activated in nearly all cells investigated from retinas 3 and 4 days after BRVO (Fig. 3D). Membrane capacitance, measured in whole-cell patch-clamp recordings, is a marker of cell membrane area. The mean membrane capacitance of Müller cells was significantly increased after 3 and 4 days of BRVO compared with cells from control tissues (Fig. 3E), suggesting that Müller cells exhibit cellular hypertrophy after BRVO. The data indicate that Müller cells in BRVO retinas alter their membrane characteristics as do Müller cells in animal models of pressure-induced transient retinal ischemia-reperfusion and diabetes, as previously described.^{24,27}

Immunoreactivities for GFAP and Vimentin

Upregulation of the immunoreactivity of intermediate filaments is a characteristic feature of retinal gliosis under pathologic conditions.¹⁹ In control retinal slices, the immunoreactivity of vimentin is localized to astrocytes in the nerve fiber/ganglion cell layers, to Müller cell fibers especially in the inner retina, and to the outer plexiform layer (Fig. 4). Within 3 days of BRVO, the immunoreactivity of vimentin apparently increased, particularly in the outer retina; in the inner retina, the thickened Müller cell fibers in the inner plexiform and nuclear layers reflect the hypertrophy of the cells. GFAP is localized in control retinas to astrocytes and to some Müller cell fibers in the ganglion cell and inner plexiform layers (Fig. 4). In retinal slices obtained after 3 days of BRVO, there was no general upregulation of GFAP compared with control retinal slices; instead, individual Müller cell fibers traversing the whole retinal thickness displayed immunoreactivity for GFAP. Some Müller cells displayed GFAP immunolabeling in the outer retina (surrounding sites of cystoid degeneration) and around vessels in the outer plexiform layer (Fig. 4).

Immunoreactivities for Kir4.1 and Aquaporin-4

It is suggested that Müller cells mediate retinal osmohomeostasis through a transcellular transport of potassium and water predominantly through Kir4.1 and aquaporin-4 channels.^{17,22,26} To reveal whether the decrease in Kir currents (Figs. 3A, 3B) may be caused by a mislocation of Kir4.1 protein in Müller cells, we immunostained retinal slices against Kir4.1. In slices of control retinas, the immunoreactivity for Kir4.1 was localized prominently around the blood vessels in the inner nuclear and outer plexiform layers and at the inner limiting membrane of the retina (Fig. 5), as previously described.²² This polarized distribution of Kir4.1 was lost within 3 days of BRVO; in slices of BRVO retinas, Kir4.1 immunoreactivity displayed a uniform distribution along the Müller cell fibers (Fig. 5). The data suggest that the decrease in Kir currents observed in Müller cells from BRVO retinas was, at least in part, caused by

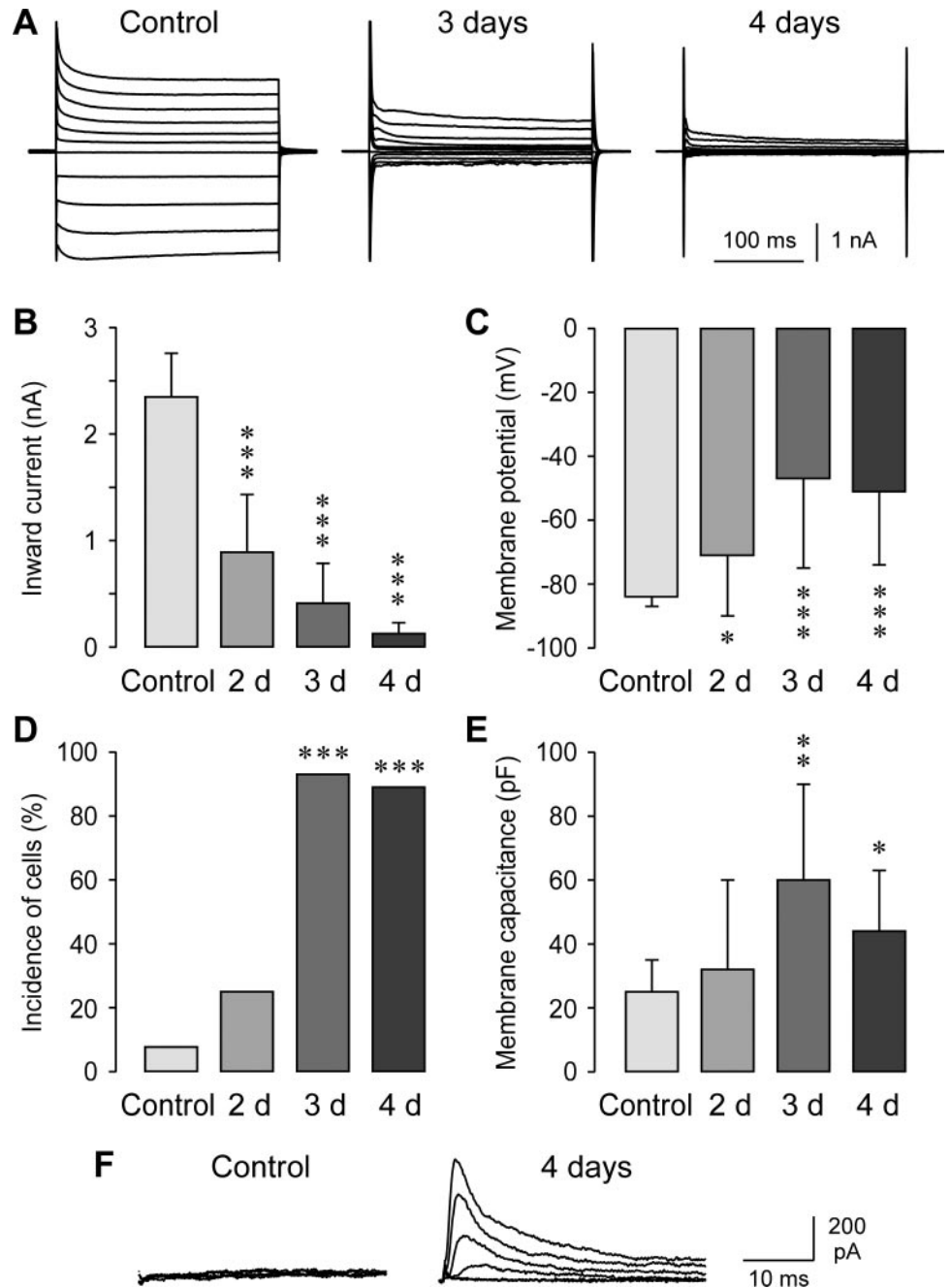


FIGURE 3. Time-dependent alterations in the potassium conductance of Müller glial cells after BRVO in the rat retina. Cells were acutely isolated from retinas after 2, 3, and 4 days of BRVO and from contralateral untreated control retinas. (A) Representative potassium current traces of cells from a control retina and retinas obtained after 3 and 4 days of BRVO. Potassium currents were evoked by 20-mV incremental voltage steps between -160 and $+40$ mV from a holding potential of -80 mV. Outward currents evoked by depolarizing voltage steps are depicted upwardly; inward currents evoked by hyperpolarizing voltage steps are depicted downwardly. (B) Mean amplitude of the inward potassium currents of Müller cells, measured at the voltage step from -80 to -140 mV. (C) Resting membrane potential. (D) Incidence of cells that displayed fast transient A-type potassium currents. (E) Cell membrane capacitance. (F) Representative current traces obtained with the difference protocol to isolate A-type potassium currents described in Materials and Methods. The cell isolated from a control retina displayed no A-type currents, whereas such currents were present in the cell obtained 4 days after BRVO. Each bar represents values obtained in 6 to 14 cells. Significant differences versus untreated control: $*P < 0.05$; $**P < 0.01$; $***P < 0.001$.

a mislocation of Kir4.1 protein associated with functional inactivation of the channels. In slices of control retinas, aquaporin-4 was localized predominantly around the vessels, at the inner limiting membrane, and in both plexiform layers (Fig. 5). The overall pattern of retinal aquaporin-4 immunostaining did not change within 3 days of BRVO, with the exception of sites of cystoid degeneration that disrupted the structure of the outer plexiform and ganglion cell layers (Fig. 5; asterisks). Cystoid spaces were regularly found in the outer plexiform layer (which contains capillaries of the outermost vascular plexus); these spaces extended into the outer nuclear layer. Cystoid spaces were also frequently found in the nerve fiber/ganglion cell layers, which contain the superficial vascular plexus. The data suggest that BRVO selectively alters the distribution of Kir4.1 protein in Müller cells, similar to the effect of pressure-induced transient retinal ischemia-reperfusion, which has been shown not to be associated with an alteration

in the localization of aquaporin-4 but with a mislocation of Kir4.1.²⁵

Swelling of Müller Cells

Cystoid degeneration of the retinal tissue is likely caused by a breakdown of the inner blood-retinal barrier and, thus, by extravasation of serum. To reveal whether cytotoxic edema resulting in cellular swelling also occurs after BRVO, we measured the cross-sectional area of Müller cell bodies located in the inner nuclear layer in freshly isolated slices of control and BRVO retinas. The mean cross-sectional area of Müller cell somata in acutely isolated retinal slices of BRVO eyes was significantly ($P < 0.05$) larger than the controls (Fig. 6A). The increase in the size of Müller cell somata might have been caused by hypertrophy and by osmotic swelling of the cells. To reveal whether the osmotic swelling properties of Müller cells

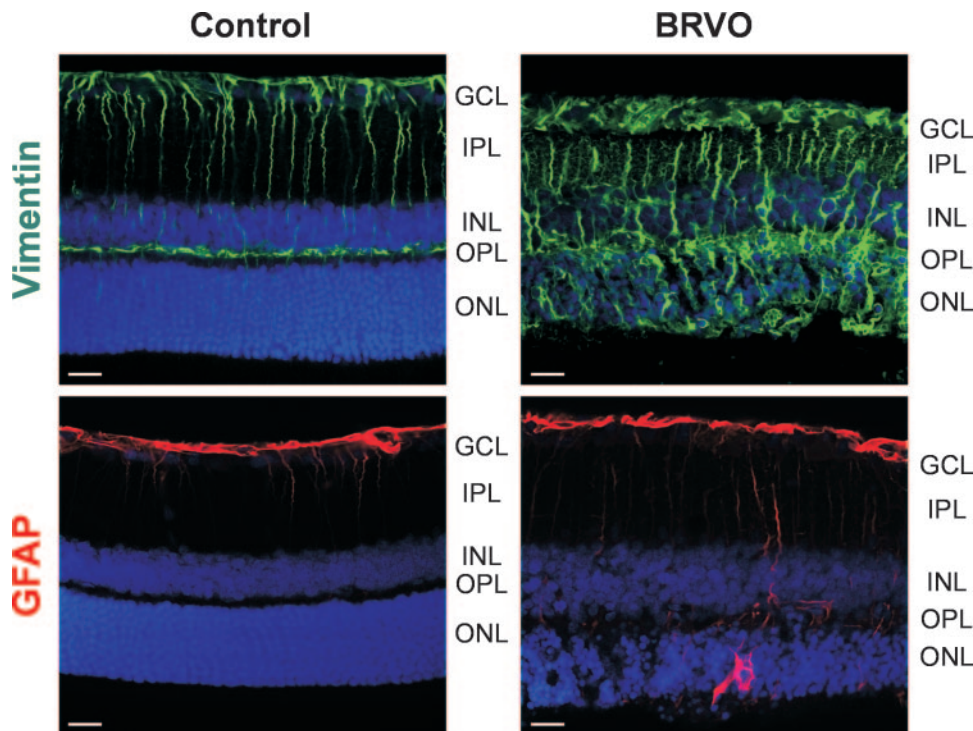


FIGURE 4. Immunolocalization of the glial intermediate filaments vimentin (*top*) and GFAP (*bottom*) in slices of a control retina and a retina obtained after 3 days of BRVO. GCL, ganglion cell layer; INL, inner nuclear layer; IPL, inner plexiform layer; ONL, outer nuclear layer; OPL, outer plexiform layer. Scale bars, 20 μ m.

are altered after BRVO, we perfused acutely isolated retinal slices with a hypoosmolar solution for 4 minutes and measured the cross-sectional area of Müller cell somata. Müller cell somata in control retinal slices did not swell under hypoosmotic stress, whereas Müller cells in slices of BRVO retinas displayed a significant ($P < 0.001$) increase somata size under these conditions (Fig. 6B). The data suggest that the rapid water transport across Müller cell membranes was altered after BRVO, resulting in cellular swelling under osmotic stress conditions.

To reveal the mechanisms of Müller cell swelling, we pre-treated the slices with blocking substances. Inhibition of the activation of phospholipase A_2 prevented the osmotic swelling of Müller cell somata in slices of BRVO retinas; similarly, inhibition of the activation of cyclooxygenase or administration of a reducing agent prevented swelling (Fig. 6B). The data suggest that oxidative stress and formation of inflammatory lipid mediators (arachidonic acid, prostaglandins) are causative factors of osmotic Müller cell swelling. This assumption is supported by the observation that Müller cell somata in control retinal slices

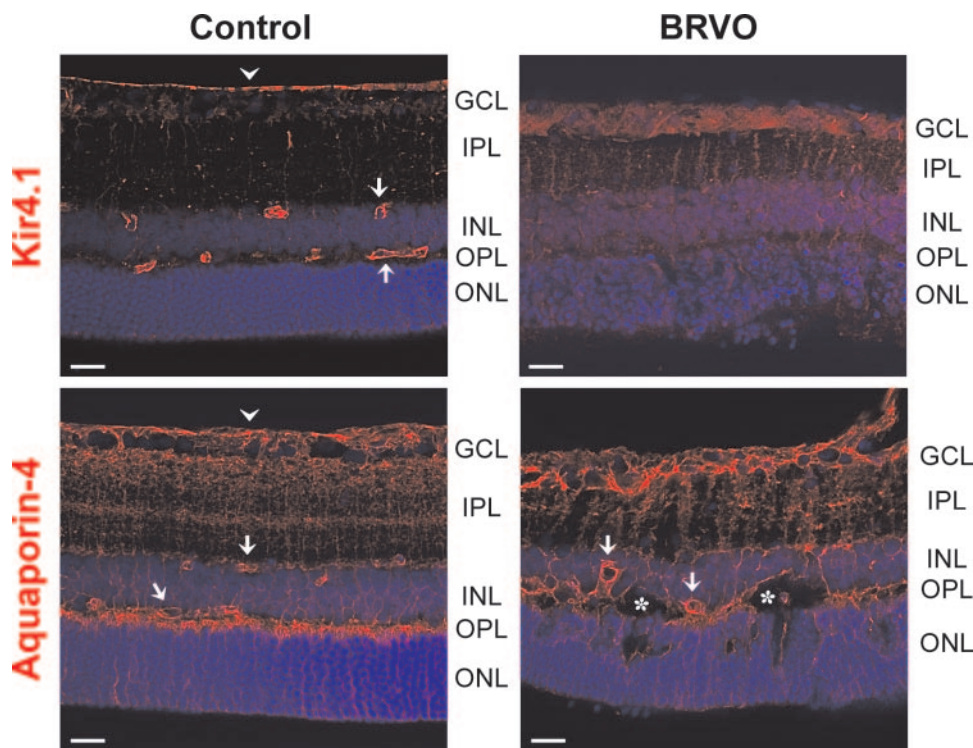
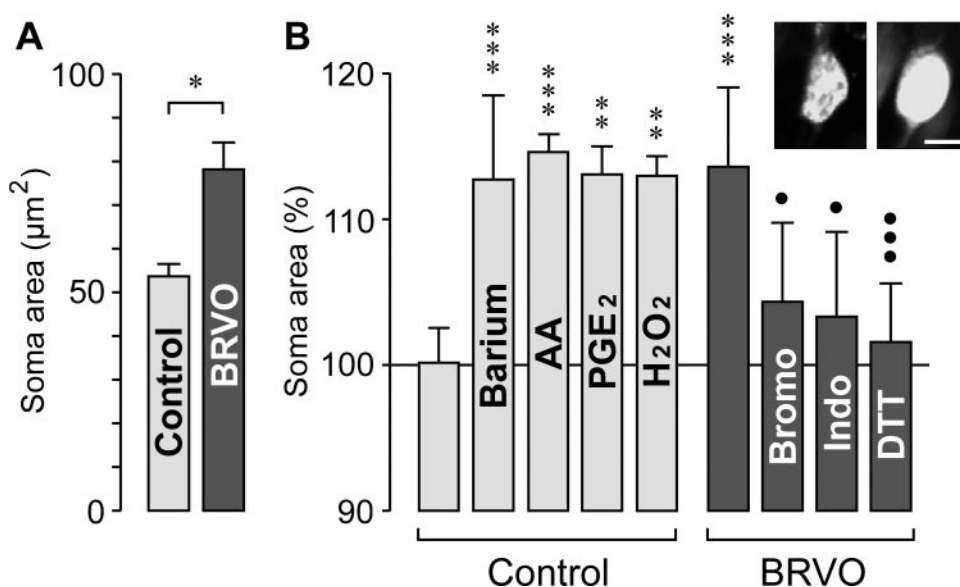


FIGURE 5. Immunolocalization of Kir4.1 and aquaporin-4 in retinal slices. In the control tissue, the Kir4.1 protein (*top row*) is concentrated at the inner limiting membrane (*arrowhead*) and around the blood vessels (*arrows*). This prominent localization is lost within 3 days of BRVO. The localization of aquaporin-4 (*bottom row*) remained unaltered within 3 days of BRVO, with the exception of sites with cystoid degeneration (*asterisks*) that disrupted the regular structure of the outer plexiform (OPL). Cell nuclei were labeled with Hoechst 33258 (*blue*). GCL, ganglion cell layer; INL, inner nuclear layer; IPL, inner plexiform layer; ONL, outer nuclear layer. Scale bars, 20 μ m.

FIGURE 6. Alterations in the soma size and osmotic swelling properties of Müller glial cells after BRVO. Data were obtained 3 days after BRVO. (A) Mean cross-sectional area of Müller cell somata in acutely isolated retinal slices from control and BRVO eyes. * $P < 0.05$. (B) Relative cross-sectional area of Müller cell somata measured after 4-minute perfusion of retinal slices with a hypoosmolar solution (containing 60% of control osmolarity). Data were obtained in retinal slices from control and BRVO eyes and are expressed in percentage of the control value obtained before osmotic challenge (100%). Cells in control retinal slices did not swell under hypoosmotic conditions. However, addition of barium chloride (1 mM), arachidonic acid (AA; 10 μ M), prostaglandin E₂ (PGE₂; 30 nM), and hydrogen peroxide (H₂O₂; 50 μ M), respectively, to the hypoosmolar solution resulted in swelling of the Müller cell bodies in control retinal slices. Cells in retinal slices from BRVO eyes displayed swelling of their somata under hypoosmotic conditions. Swelling was inhibited in the presence of the following agents: the selective inhibitor of phospholipase A₂ activation 4-bromophenacyl bromide (bromo; 300 μ M), the cyclooxygenase inhibitor indomethacin (indo; 10 μ M), and the cell-permeable reducing agent dithiothreitol (DTT; 3 mM), respectively. Images display original records of a dye-filled Müller cell body recorded before (*left*) and during (*right*) hypoosmotic exposure. Scale bars, 5 μ m. Each bar represents values obtained in 6 to 50 cells. Significant differences compared with control (100%): ** $P < 0.01$; *** $P < 0.001$. Significant blocking effects: ● $P < 0.05$; ●●● $P < 0.001$.



displayed osmotic swelling in the presence of arachidonic acid, prostaglandin E₂, or hydrogen peroxide (Fig. 6B). The fact that Müller cell somata in control retinal slices displayed swelling in the presence of the Kir channel blocker barium chloride (Fig. 6B) suggests that the functional inactivation of Kir channels is another causative factor of Müller cell swelling in BRVO retinas.

DISCUSSION

In the present study using a rat model of laser-induced BRVO, we describe alterations in retinal gene expression of factors and channels implicated in the development/resolution of retinal edema. In addition, we describe alterations in the physiological properties of Müller cells that likely contribute to a disturbance of the retinal osmohomeostasis and an impairment of fluid absorption from the edematous retinal tissue.

Alterations in Retinal Gene Expression

We found that VEGF is rapidly upregulated in the neuroretina after BRVO; the expression of VEGF returned to control level within 3 days of BRVO. The rapid upregulation of VEGF may represent one major factor that contributes to the breakdown of the inner blood-retinal barrier resulting in the formation of cystoid spaces around retinal vessels. The normalization of the VEGF expression after 3 days of BRVO may be caused (at least in part) by PEDF, which was upregulated at this time; PEDF is a known negative regulator of VEGF expression.^{10,11} In contrast to VEGF, which was upregulated only in the neuroretina and not in the retinal pigment epithelium, PEDF was upregulated in both tissues. The reason for this difference is unclear; the production of the neuroprotective factor PEDF in the retinal pigment epithelium may be increased in response to the degenerative stress of photoreceptors around the cystoid spaces in the outer retina. The upregulation of PEDF may provide an antiangiogenic environment in the retina after BRVO. After 1 day of BRVO, the expression of PEDF in the neuroretina was unaltered compared with control. Although

some studies suggest that VEGF suppresses the release of PEDF from retinal glial cells,²⁸ the present results indicate that an elevated level of VEGF is not necessarily associated with a decrease in the expression of PEDF in the ischemic retina.

We show for the first time that prothrombin is produced in the neuroretina and the retinal pigment epithelium and that the expression of prothrombin is sensitive to retinal ischemia. Within 1 day of BRVO, the expression of prothrombin is decreased in both tissues. The reason for this downregulation is unclear and may be explained with a negative regulation by extravasated prothrombin or thrombin. Further studies are necessary to reveal the ischemic regulation of prothrombin in the retina. The unaltered expression of the tissue factor in the neuroretina suggests that the extrinsic pathway of blood coagulation is not facilitated after BRVO.

Müller Cell Gliosis

We found that BRVO is associated with a severe gliosis of Müller cells. After BRVO, Müller cells display cellular hypertrophy, an increase in vimentin labeling, a strong decrease in transmembrane potassium currents, membrane depolarization, a decrease in the gene expression of Kir4.1 and aquaporin-4, a mislocation of Kir4.1 protein in the plasma membrane, and an alteration in the osmotic swelling properties. The membrane potential of Müller cells decreased to approximately 50 mV, which is the threshold for the activation of voltage-gated, outwardly rectifying potassium channels that mediate, for example, the fast transient A-type potassium currents. Apparently, the mislocation of the Kir4.1 protein was associated with a functional inactivation of this potassium channel, reflected in the strong decrease of the transmembrane potassium currents. With respect to aquaporin-4, we found a decrease in gene expression but no overall mislocation of the protein (with the exception of sites of cystoid retinal degeneration). Similar mislocation of Kir4.1 protein and unaltered retinal distribution of aquaporin-4 protein were described in animal models of retinal ischemia-reperfusion, retinal detachment, and diabetic retinopathy.^{23,24,29} The relative independence of gene expres-

sion and protein localization was also observed with respect to Kir4.1 in the non-BRVO areas of retinas in which half the veins were occluded. Although gene expression was downregulated (Fig. 2), the localization of Kir4.1 protein in retinal slices was not altered (not shown). Gene expression of Kir4.1 and aquaporin-4 and membrane anchoring of Kir4.1 are sensitive to retinal ischemia, whereas the membrane anchoring of aquaporin-4 is insensitive to ischemia. Based on observations in knockout mice, it has been suggested that α -syntrophin (a protein of the dystrophin-associated protein complex) is implicated in the membrane anchoring of aquaporin-4 but not of Kir4.1.³⁰ The mechanism of the ischemia-sensitive membrane anchoring of Kir4.1 remains to be determined.

Dysfunction of Müller Cells

Inactivation and downregulation of Kir4.1 channels likely result in an impairment of the retinal potassium and water homeostasis normally mediated by Müller cells. Elevation in the interstitial potassium level contributes to neuronal hyperexcitation and glutamate toxicity. Membrane depolarization after functional inactivation of Kir4.1 decreases the efficiency of electrogenic neurotransmitter transporters such as for glutamate. Inactivation of Kir4.1 channels causes uncoupling of the aquaporin-4-mediated water transport from the potassium currents, resulting in alteration of the water movement across the interfaces of Müller cells and extraretinal fluid-filled spaces (blood vessels, vitreous). Water (derived from extravasated serum and from the oxidative metabolism of the retina) cannot be cleared into the blood and accumulates in the retinal tissue. Increases in the osmotic pressure of Müller cells and the retinal interstitium (e.g., after accumulation of potassium ions) drives water from the vessels into the retinal parenchyma, resulting in cystoid degeneration around the vessels. Thus, a disturbance of the transglial water transport resulting in impaired fluid absorption from the retinal tissue may contribute to the development of edema after BRVO.

Spread of Müller Cell and Retinal Responses

We found that alterations in retinal gene expression are not restricted to the vein-occluded retinal areas but are also observed in the neighboring nonoccluded tissue. A similar spread of elevated expression of inflammation- and immune response-related genes into the surrounding nonaffected tissue was recently described in an animal model of focal retinal detachment.³¹ It is likely that proinflammatory factors such as VEGF, blood-derived factors, and reactive oxygen radicals diffuse from the vein-occluded into the surrounding tissue, resulting in reactive gliosis and alterations in gene expression. It has been shown in a rat model of BRVO that retinal hemorrhage is limited to the vein-occluded retinal regions, whereas edema occurs also in the neighboring nonoccluded regions.³² The downregulation of potassium and water channels suggests that the Müller cell-mediated osmohomeostasis may be disturbed (in a delayed fashion) in the entire retinal tissue, resulting in neuronal dysfunction also in nonoccluded retinal areas.

Conclusions

The present results may have some implications for an understanding of the clinical situation. Because of the rapid upregulation of VEGF, VEGF inhibitors should be administered in a very short interval after the onset of vein occlusion. PEDF may protect cells in the ischemic retina from death, contributing to the relatively good prognosis for patients with BRVO.² Retinal edema in patients with BRVO is presumably caused by vascular leakage and impairment in the Müller cell-mediated fluid absorption from the tissue. Fluid absorption is not improved by anti-VEGF therapies but is suggested to be stimulated by tri-

amcinolone acetonide.³³ Triamcinolone was shown to prevent the osmotic swelling of Müller cells through an opening of potassium and chloride channels in the Müller cell membranes.³³

Acknowledgments

The authors thank Ute Weinbrecht for excellent technical support.

References

- Finkelstein D. Ischemic macular edema: recognition and favorable natural history in branch vein occlusion. *Arch Ophthalmol*. 1992; 110:1427-1434.
- Rehak J, Rehak M. Branch retinal vein occlusion: pathogenesis, visual prognosis, and treatment modalities. *Curr Eye Res*. 2008;33: 111-131.
- Branch Retinal Vein Occlusion Study Group. Argon laser photocoagulation for macular edema in branch vein occlusion. *Am J Ophthalmol*. 1984;98:271-282.
- Pe'er J, Shweiki D, Itin A, Hemo I, Gnessin H, Keshet E. Hypoxia-induced expression of vascular endothelial growth factor by retinal cells is a common factor in neovascularizing ocular diseases. *Lab Invest*. 1995;72:638-645.
- Aiello LP, Bursell SE, Clermont A, et al. Vascular endothelial growth factor-induced retinal permeability is mediated by protein kinase C in vivo and suppressed by an orally effective beta-isoform-selective inhibitor. *Diabetes*. 1997;46:1473-1480.
- Adamis AP, Shima DT. The role of vascular endothelial growth factor in ocular health and disease. *Retina*. 2005;25:111-118.
- Noma H, Funatsu H, Yamasaki M, et al. Pathogenesis of macular edema with branch retinal vein occlusion and intraocular levels of vascular endothelial growth factor and interleukin-6. *Am J Ophthalmol*. 2005;140:256-261.
- Wu L, Arevalo JF, Roca JA, et al. Comparison of two doses of intravitreal bevacizumab (Avastin) for treatment of macular edema secondary to branch retinal vein occlusion: results from the Pan-American Collaborative Retina Study Group at 6 months of follow-up. *Retina*. 2008;28:212-219.
- Campochiaro PA, Hafiz G, Shah SM, et al. Ranibizumab for macular edema due to retinal vein occlusions: implication of VEGF as a critical stimulator. *Mol Ther*. 2008;16:791-799.
- Zhang SX, Wang JJ, Gao G, Parke K, Ma JX. Pigment epithelium-derived factor downregulates vascular endothelial growth factor (VEGF) expression and inhibits VEGF-VEGF receptor 2 binding in diabetic retinopathy. *J Mol Endocrinol*. 2006;37:1-12.
- Yamagishi S, Nakamura K, Matsui T, et al. Pigment epithelium-derived factor inhibits advanced glycation end product-induced retinal vascular hyperpermeability by blocking reactive oxygen species-mediated vascular endothelial growth factor expression. *J Biol Chem*. 2006;281:20213-20220.
- Derevjanik NL, Vinos SA, Xiao WH, et al. Quantitative assessment of the integrity of the blood-retinal barrier in mice. *Invest Ophthalmol Vis Sci*. 2002;43:2462-2467.
- Sakamoto T, Sakamoto H, Sheu SJ, Gabrielian K, Ryan SJ, Hinton DR. Intercellular gap formation induced by thrombin in confluent cultured bovine retinal pigment epithelial cells. *Invest Ophthalmol Vis Sci*. 1994;35:720-729.
- Bian ZM, Elner SG, Elner VM. Thrombin-induced VEGF expression in human retinal pigment epithelial cells. *Invest Ophthalmol Vis Sci*. 2007;48:2738-2746.
- Walsh PN, Ahmad SS. Proteases in blood clotting. *Essays Biochem*. 2002;38:95-111.
- Mori F, Hikichi T, Takahashi J, Nagaoka T, Yoshida A. Dysfunction of active transport of blood-retinal barrier in patients with clinically significant macular edema in type 2 diabetes. *Diabetes Care*. 2002;25:1248-1249.
- Bringmann A, Reichenbach A, Wiedemann P. Pathomechanisms of cystoid macular edema. *Ophthalmic Res*. 2004;36:241-249.
- Pederson JE. Fluid physiology of the subretinal space. In: Wilkinson CP, ed. *Retina*. St Louis: Mosby-Year Book; 1994:1955-1968.
- Bringmann A, Pannicke T, Grosche J, et al. Müller cells in the healthy and diseased retina. *Prog Retin Eye Res*. 2006;25:397-424.

20. Stamer WD, Bok D, Hu J, Jaffe GJ, McKay BS. Aquaporin-1 channels in human retinal pigment epithelium: role in transepithelial water movement. *Invest Ophthalmol Vis Sci.* 2003;44:2803-2808.
21. Iandiev I, Pannicke T, Reichel MB, Wiedemann P, Reichenbach A, Bringmann A. Expression of aquaporin-1 immunoreactivity by photoreceptor cells in the mouse retina. *Neurosci Lett.* 2005;388:96-99.
22. Nagelhus EA, Horio Y, Inanobe A, et al. Immunogold evidence suggests that coupling of K⁺ siphoning and water transport in rat retinal Müller cells is mediated by a coenrichment of Kir4.1 and AQP4 in specific membrane domains. *Glia.* 1999;26:47-54.
23. Pannicke T, Iandiev I, Uckermann O, et al. A potassium channel-linked mechanism of glial cell swelling in the postischemic retina. *Mol Cell Neurosci.* 2004;26:493-502.
24. Pannicke T, Iandiev I, Wurm A, et al. Diabetes alters osmotic swelling characteristics and membrane conductance of glial cells in rat retina. *Diabetes.* 2006;55:633-639.
25. Uckermann O, Iandiev I, Francke M, et al. Selective staining by vital dyes of Müller glial cells in retinal wholemounts. *Glia.* 2004;45:59-66.
26. Kofuji P, Ceelen P, Zahs KR, Surbeck LW, Lester HA, Newman EA. Genetic inactivation of an inwardly rectifying potassium channel (Kir4.1 subunit) in mice: phenotypic impact in retina. *J Neurosci.* 2000;20:5733-5740.
27. Pannicke T, Uckermann O, Iandiev I, et al. Altered membrane physiology in Müller glial cells after transient ischemia of the rat retina. *Glia.* 2005;50:1-11.
28. Eichler W, Yafai Y, Keller T, Wiedemann P, Reichenbach A. PEDF derived from glial Müller cells: a possible regulator of retinal angiogenesis. *Exp Cell Res.* 2004;299:68-78.
29. Iandiev I, Uckermann O, Pannicke T, et al. Glial cell reactivity in a porcine model of retinal detachment. *Invest Ophthalmol Vis Sci.* 2006;47:2161-2171.
30. Puwarawuttipanit W, Bragg AD, Frydenlund DS, et al. Differential effect of α -syntrophin knockout on aquaporin-4 and Kir4.1 expression in retinal macroglial cells in mice. *Neuroscience.* 2006;137:165-175.
31. Hollborn M, Francke M, Iandiev I, et al. Early activation of inflammation- and immune response-related genes after experimental detachment of the porcine retina. *Invest Ophthalmol Vis Sci.* 2008;49:1262-1273.
32. Zhang Y, Fortune B, Atchaneeyasakul LO, et al. Natural history and histology in a rat model of laser-induced photothrombotic retinal vein occlusion. *Curr Eye Res.* 2008;33:365-376.
33. Uckermann O, Kutzera F, Wolf A, et al. The glucocorticoid triamcinolone acetonide inhibits osmotic swelling of retinal glial cells via stimulation of endogenous adenosine signaling. *J Pharmacol Exp Ther.* 2005;315:1036-1045.